Research Square

Preprints are preliminary reports that have not undergone peer review.
They should not be considered conclusive, used to inform clinical practice,
or referenced by the media as validated information.

Parkin-mediated transcriptional regulation of inducible NO-synthase impacts microglial inflammatory response in Parkinson disease-related cells and mice models

Julien Minniti
Université Côte d'Azur
Maria Eduarda Bianchetti
Universidade de São Paulo
Ligia Ramos dos Santos
Université Côte d'Azur
Aurore Bernardin
Université Côte d'Azur
Charlotte Bauer
Université Côte d'Azur
Henri Le Bihan
Université Côte d'Azur
Luis Roberto Britto
Universidade de São Paulo
Frédéric Checler
Université Côte d'Azur
Eric Duplan
Université Côte d'Azur
Cristine Alves da Costa
acosta@ipmc.cnrs.fr

Université Côte d'Azur

Article

Keywords:

Posted Date: November 11th, 2026

DOI: https://doi.org/10.21203/rs.3.rs-11501392/v1

License: This work is licensed under a Creative Commons Attribution 4.0 International License.
Read Full License

Additional Declarations: No competing interests reported.

Parkin-mediated transcriptional regulation of inducible NO-synthase impacts microglial inflammatory response in Parkinson disease-related cells and mice models.

Julien Minniti[1], Maria Eduarda Bianchetti[2], Ligia Ramos dos Santos[1], Aurore Bernardin[1], Charlotte Bauer[1], Henri Le Bihan[1], Luis Roberto Britto[2], Frédéric Checler[1], Eric Duplan[1]* and Cristine Alves da Costa[1]*

1- University Côte d'Azur, INSERM U1323**,** CNRS UMR7275, Institut de Pharmacologie Moléculaire et Cellulaire (IPMC), team label "Laboratory of Excellence (LABEX) Distalz", 06560, Valbonne, France.

2- Department of Physiology and Biophysics, Institute of Biomedical Sciences, University of São Paulo, São Paulo, Brazil.

*Correspondence should be addressed to CAC, acosta@ipmc.cnrs.fr, or ED duplan@ipmc.cnrs.fr IPMC, Sophia-Antipolis, Valbonne, France.

ABSTRACT

Neuroinflammation and oxidative stress are central to the pathogenesis of Parkinson disease (PD). inducible Nitric Oxide Synthase (iNOS), via excessive nitric oxide (NO) production, drives dopaminergic neurodegeneration. While Parkin, an E3 ubiquitin ligase mutated in familial PD, is renowned for its role in mitochondrial quality control. Emerging evidence suggests that it also functions as a transcriptional factor. However, its involvement in neuroinflammatory pathways at the transcriptional level remains poorly understood.

In this study, we investigate the role of parkin-associated transcriptional function in the control of neuroinflammation in human microglial HMC3 cells as well as in the paraquat-induced sporadic Parkinson disease mouse model. We demonstrate that parkin modulates microglial activation by regulating human and mice cell proliferation and NO production. Parkin deficiency exacerbates iNOS induction and NO release. Mechanistic analysis indicates that parkin directly binds the *iNOS* promoter, thereby suppressing its transcription. Parkin expression rescue attenuates iNOS activation, thus confirming its protective role. Notably, we reveal a feedback loop wherein iNOS mediates parkin nitrosylation, suggesting a functional cross-talk between these two proteins. Furthermore, the anti-inflammatory properties of parkin, both *in vitro* and *in vivo,* were strengthened by its ability to modulate both central and peripheral cytokines production in mice. Of importance, we show that endogenous parkin depletion increases iNOS mRNA levels, a phenotype fully abolished by the Parkinson disease-like inducing toxin paraquat.

Overall, our study uncover a novel function of parkin as a transcriptional repressor of *iNOS*, that could explain the putative link between mitochondrial dysfunction, microglial activation, and nitrosative stress in PD. Targeting the parkin-iNOS axis may thus offer an original alternative potential therapeutic strategy to curb neuroinflammation and slow disease progression in Parkinson Disease.

43 **ABBREVIATIONS**

44

1-methyl-4-phenyl-1,2,3,6-tetrahydropyridine	MPTP
6-hydroxydopamine	6-OHDA
Bovine serum albumin	BSA
Damage Associated Molecular Pattern	DAMPS
Electrophoretic Mobility Shift Assay	EMSA
Empty vector	EV
Fetal bovine serum	FBS
Glyceraldehyde-3-Phosphate Dehydrogenase	GAPDH
HEPES, EDTA, Neocuproine	HEN
HEPES, EDTA, Neocuproine, protease inhibitor	HENP
Human microglial cell line	HMC3
inducible NO-synthase	iNOS
inhibitor of KB kinase	IKKγ/NEMO
Interleukine	IL
lipopolysaccharide	LPS
Neuroinflammation	NIF
neuronal NO-synthase	nNOS
nitric oxide	NO
NOD-like receptor family, pyrin domain containing 3	NLRP3
nuclear factor-kappa B	NFKB
Parkin	PK
Parkinson disease	PD
PK responsive element	PKRE

presenilins 1 and 2	PS1 / PS2
Reactive oxygen species	ROS
Receptor interacting serine/threonine kinase 1	RIPK1
S-Methyl methanethiosulfonate	MMTS
S-nitrosothiol (SNO)-Resin Assisted Capture	SNO-RAC
Sodium dodecyl sulfate	SDS
TNF receptor-associated factor 2	TRAF2
Toll-like receptor 4	TLR4
Transcription Start Site	TSS
Transcriptional factor	TF

45

46

INTRODUCTION

Parkinson disease (PD) is the second most common neurodegenerative disorder. It is characterized by motor disability linked to the progressive degeneration of dopaminergic neurons. PD represents a major public health problem and economic burden that should likely worsens according to its growing prevalence in the aging population. Thus, deciphering the molecular cascades responsible for the selective neuronal death underlying its progression is of paramount importance.

Over the past decade, research into PD pathophysiology has revealed multiple interconnected dysfunctional processes. Among them, neuroinflammation (NIF) has emerged as a key pathogenic defect occurring early in PD. Compelling pre-clinical and clinical evidences support a critical role for both innate and adaptive immunity contributing to, and being activated in response to nigrostriatal injury [1].

PD can be of sporadic or genetic origins, but both forms appear mechanistically intertwined. Thus, studying the role of PD-causative gene products can help to understand the etiology of sporadic PD. Parkin (PK), a major PD-causative gene, was initially characterized as an E3 ubiquitin ligase, the loss of function of which directly leads to the accumulation of potentially toxic proteins due to the impairment of their proteasomal degradation [2]. However, we and others have uncovered an additional role for PK as a transcriptional regulator (TF)**.** We previously demonstrated that PK represses the pro-apoptotic tumor suppressor *p53* gene by physically interacting with its promoter [3], a function abolished by PD-linked mutations. This seminal finding was later confirmed by Sunico et al. [4] who also showed that both PK TF activity and nuclear translocation can be impaired by its S-nitrosylation. Subsequently, we identified two additional PK targets, presenilin 1 (PS1) and presenilin 2 (PS2)**,** allowing us to define a consensus binding motif for PK [5].

Intriguingly, PK plays a pivotal role in modulating NIF through multiple mechanisms, including mitochondrial quality control and downstream innate immune signaling pathways. Its involvement in controlling neuroinflammation is multifactorial, implying a complex interplay between mitophagy, inflammasome activation, glial cell-linked phenotypes, and the transcriptional regulation of immune responses [5-10].

In partnership with PINK1, PK regulates mitophagy, thereby controlling the release of mitochondrial damage-associated molecular patterns (DAMPs) that modulate the innate immune response, notably via the cGAS-STING pathway and NLRP3 inflammasome activation[5, 6, 11]. PK also participates in the ubiquitination and degradation of NLRP3 in microglial and neuronal cells, leading to a reduction in the secretion of pro-inflammatory cytokines such as IL-18 and IL-1β [7, 12]. Furthermore, PK regulates the transcription and translation of A20, an inhibitor of the pro-inflammatory Toll-like receptor 4 (TLR4) [8] which is involved in NF-κB p65 activation. Notably, PK can directly activate NF-κB, a master regulator of inflammation, through its interactions with IKKγ/NEMO, TRAF2, and RIPK1 [13-15] suggesting that PK is not merely an inhibitor of NIF but also a contextual modulator of immune homeostasis.

Despite these advances, most studies on PK role in NIF have focused on its E3 ligase activity, leaving its transcriptional regulatory functions underexplored. Here, we address this critical gap by investigating PK TF-mediated control of inducible nitric oxide synthase (iNOS)**,** an enzyme at the center of gravity of neuroinflammation process. This choice was motivated by two key observations: first, PK undergoes nitrosylation [16], a modification dependent on nitric oxide (NO) produced by nitric oxide synthases, including iNOS and nNOS; second, PK nitrosylation impairs both its E3 ligase [16] and TF functions [4]. We therefore hypothesized that a bidirectional functional regulatory loop between PK and iNOS may contribute to the control of neuroinflammation in PD.

In this study, we demonstrate that PK regulates the proliferation, phagocytosis, and NO production of microglial cells of both mouse and human origin. We provide evidence that PK directly regulates *iNOS* transcription by binding to its promoter and that iNOS, in turn, nitrosylates PK in human microglial HMC3 cells. Additionally, we show that PK modulates cytokine levels in both the central nervous system and the periphery. Using a paraquat-induced neurotoxic lesion PD model, we further reveal that the depletion of endogenous PK leads to increased iNOS expression in aged mice, an effect that is abrogated by paraquat administration.

Collectively, our findings demonstrate a novel role for PK TF function in controlling neuroinflammation in both a human *in vitro* microglial cell models as well as *in vivo*, in a paraquat-induced sporadic PD model.

MATERIALS AND METHODS

Cellular models

Human HMC3 (ATCC CRL-3304) and mouse BV2 were cultured in Dulbecco's Modified Eagle's Medium (DMEM) supplemented with fetal bovine serum (FBS, 10%), penicillin (100 U/mL) and streptomycin (50 µg/mL) and incubated at 37 °C in a 5% CO_2 atmosphere. HMC3 and BV2 stably overexpressing wild-type human PK were obtained by co-transfection of 1.9 µg of pSBbi-Pur PK (or pSBbi-Pur (empty vector EV)) (Addgene plasmid #60523) and 100 ng of pCMV(CAT)T7-SB100 (Addgene plasmid # 34879) in 6-well plates using the jetPRIME transfection reagent according to the manufacturer's protocol (Polyplus). To obtain HMC3 double transfectant models (EV (empty vector)/EV, EV/PK, iNOS/EV, iNOS/PK), we performed a co-transfection 0.950 µg of pSBtet-Pur iNOS (or pSBtet-Pur) (Addgene Plasmid #60507**)**, 0.950 µg of pSBbi-Pur PK (or pSBBi-Pur) and 100 ng of pCMV(CAT)T7-SB100. The plasmid pSBtet-Pur is a Tet-ON doxycycline inducible plasmid. Twenty-four hours after transfection, cells were treated with puromycin (1 µg/mL) and selection was carried out for one week. Cells were trypsinized and polyclonal populations were maintained in the presence of the corresponding selection drug.

Transitory transfections and treatments

Transitory transfections were made by means of JetPRIME (Polyplus, Illkirch , France) reactive according to the manufacturer's protocol. In brief, cells were transfected overnight with 2 µg of DNA before treatments.

In a subset of experiments BV2 (200000 cells) and HCM3 (200000 cells) control or overexpressing PK were plated in 6-well plates and cultivated as above till reaching 80% confluence. Then, they were treated with lipopolysaccharide (LPS) (1 µg/mL, L4391; Sigma-Aldrich, Saint-Louis, Missouri, USA). In nitrosylation studies, PK/iNOS stable HCM3 transfectant models were treated with or without doxycycline (1 µM, D5207, Sigma-Aldrich).

Western Blot

HMC3, BV2, or mice striatum were lysed in RIPA and sonicated. Samples (50µg of total proteins) were loaded on 8%-12% PROTEAN TGX stain-free mini gels (1.5mm) and semi-dry transferred for 10 min by means of the precut blotting transfer pack (1704271, Bio Rad, Hercules, California, USA) and the Trans-Blot® Turbo™ Transfer System using a pre-programmed protocol. Transferred proteins were blocked in 5% non-fat milk (phosphate buffered saline, PBS) for one hour and immuno-blotted with anti-PK (clone PRK8 Millipore MAB 5512, dilution 1:1000), anti-GAPDH (clone 6C5 Millipore MAB 374, dilution 1:1000), anti-mouse iNOS (D6B6S, Rabbit mAb Cell Signaling 13120, dilution 1:1000), anti-IL1β (Sigma-Aldrich I3767, dilution 1:1000) antibodies. Membranes used for immunoblotting of human iNOS were blocked with 5% BSA (bovine serum albumin, A9647, Sigma-Aldrich) diluted in TBS (Tris Buffered Saline) and immuno-blotted with anti-human iNOS (E3W6B, Rabbit mAb Cell Signaling 20609, dilution 1:1000). All primary antibodies were incubated over-night at 4°C. According to primary antibody used, immunological complexes were revealed with anti-rabbit, anti-mouse, or anti-goat, IgG-coupled peroxidase antibodies (Jackson ImmunoResearch, dilution 1:5000) by the electrochemiluminescence detection method (K-12043-D20, Advansta, San Jose, California, USA). Chemiluminescence was recorded using a luminescence image analyzer ChemiDoc™ Imaging System (Bio Rad) and quantifications of non-saturated images were performed with the Image lab 6.0.1 software. The utilization of stain-free imaging also allows normalization of bands of interest to total proteins loaded in each lane. All full gels are provided as a supplementary figure.

Real Time proliferation assay

The xCELLigence technology (ACEA Biosciences Inc.) allows the Real Time Cell Analysis (RTCA) of cell proliferation without chemical interference. The RTCA instrument was used to assess the proliferation of different cell models overexpressing PK. All the experiments have been done after a titration assay that allowed us to determine the optimal cell seeding density for each cell line (10000 cells for BV2, 20000 cells for HMC3). After an automatic scan of the plate to check for proper contact of the E-plate, the background impedance for each well of the plate was measured before the cells were

plated and incubated for 30 min at 37 °C and 5% CO_2 to allow their settling in an evenly distributed pattern. The E-plate 16 was then put in the cradle pocket of the RTCA apparatus, and the data acquisition was initiated. The impedance signals were recorded every 5 min for the first 25 scans (2 h) and every 15 min until the end of the experiment (up to 72 h).

Cell cycle analysis by Flow Cytometry

HMC3 and BV2 cells were grown in six-well plates in DMEM media containing 10% FBS. To synchronize the cells, BV2 and HCM3 were cultured at 37 °C for 24 hours in DMEM medium containing 0,1% FBS, then returned to normal culture conditions (10% FBS) for 24 hours to stimulate cell re-entry into the cell cycle. Cells were harvested, pelleted by centrifugation at 1,000 × g for 10 min at 4 °C, fixed with 80% ice-cold ethanol (in PBS buffer) under slow vortex agitation, chilled on ice for one hour, pelleted and gently diluted in 500 µL of PBS containing propidium iodide (50 µg/mL, S7109, Sigma-Aldrich) and RNAse A (1 mg/mL, R6513, Sigma Aldrich) and then incubated at 37 °C for 30 minutes. The PI fluorescence of individual nuclei was measured by using a FACScan flow cytometer (ACEA BIO, NovoCyte Flow Cytometer, 488 nm laser line, for excitation). Red fluorescence due to PI staining of DNA was expressed on a logarithmic scale simultaneously to the forward scatter of the particles. Fifty thousand events were counted on the scatter gate. All measurements were performed under identical conditions. Data analysis was performed by means of the NOVOEXPRESS™ software.

Phagocytosis assays

To evaluate phagocytosis, HMC3 cells, overexpressing or not PK, were seeded at a rate of 2×10^5 cells per well in 6-well plates. After 24 hours, the cells were stimulated overnight with LPS (1 µg/mL). Next, latex beads, amine-modified polystyrene, fluorescent red (L2778, Sigma-Aldrich) were added for 4 hours at 1/1000 after a “pre-opsonization” during 1 hour at 1 vol. of beads for 4 vol. of FBS. The cells were then washed five times with 1X PBS to remove non-internalized particles, then detached using Accutase (A6964-100ml, Sigma-Aldrich). Finally, the cell suspensions were analyzed by flow cytometry (Cytek Aurora Spectral Flow Cytometry).

Nitric Oxide production

To determine NO levels, BV2 cells (200000 cells) were cultured in DMEM/F-12 media without phenol red. Following LPS treatment, 200 µL of the culture medium was recovered and incubated with 100 µL of reagent A (1% (w/v) sulfanilamide in 5% phosphoric acid) for 10 minutes at room temperature in the dark. Then, 100 µL of reagent B (0.1% (w/v) N-(1-naphthyl)-ethylenediamine dihydrochloride (NED)) was added to the reaction mixture, which was then incubated for a further 10 minutes at room temperature in the dark. Then, 100 µL of the sample was placed in a 96-well plate. Absorbance was measured at 543 nm for 30 minutes using a plate reader (Spectral Scanning Multimode Reader Varioskan™ Flash, Thermo Scientific, Waltham, Massachusetts, USA). A calibration curve of sodium nitrite (0-100 µM) was used for quantification.

S-nitrosothiol (SNO)-Resin Assisted Capture (SNO-RAC)

The precipitation protocol for S-nitrosylated proteins is based on that described by [17]. All steps are performed away from direct light. In brief, the thiopropyl sepharose 6B resin (786-1785, G-BIOSCIENCES, Saint-Louis, Missouri, USA) is hydrated with a 50% HEN (250 mM HEPES, 1 mM EDTA, 0.1 mM Neocuproine (N1501, Sigma-Aldrich)) slurry buffer. For each condition, double stable HMC3 cells was plated in two 150 mm-diameters. The cell pellet is snap-frozen twice in dry ice in HEN buffer containing protease inhibitors (HENP, protease inhibitors from P2714, Sigma-Aldrich), then sonicated four times for 20 seconds. The free thiol groups are then blocked in a 50 °C water bath for 30 minutes (mixed by vortexing at 5-minute intervals) in a solution of HENP, 2.5% SDS (sodium dodecyl sulfate) and 0.15% MMTS (*S*-Methyl methanethiosulfonate, 208795, Sigma-Aldrich). The proteins are then precipitated with 100% ice-cold acetone and incubated overnight at -30°C. The protein pellet is then washed with 70% acetone and resuspended in HEN buffer containing 1% SDS. The blocked proteins are then incubated overnight at room temperature in a tube rotor, either with or without 500 mM ascorbic acid (Asc, 11140, Sigma-Aldrich) and with resin. Without ascorbic acid, nitrosylated proteins cannot bind to the resin; this is the negative control. The resin pellet is then washed with HENS

and the proteins bound to the resin are eluted with 1X loading buffer containing 10% β-mercaptoethanol and analyzed by conventional Western blot.

iNOS promoter cloning and mutagenesis

The human promoter of iNOS was cloned from genomic DNA of HMC3 with 5'-CGACGCGCCCTTC CCTTCCCTTTCTTTC-3' MluI forward primer (-1015 from ATG) and 5'-CCCTCGAGCTCTATGGC TTTACAAAGCAGGTC-3' XhoI reverse primer into a pGL3-basic-luciferase vector. Deletion of PKRE (+1290 from TSS) was performed by site directed mutagenesis by means of the 5'-GGCACCCCTGTTTCAACGACCTGCTCTTCCTCACCCTGCCTGTG-3' forward and 5'-CACA GGCAGGGTGAGGAAGA GCAGGTCGTTGAAACA GGGGTGCC-3' reverse primers.

iNOS promoter activity

HMC3 overexpressing or not PK were seeded in six-well plates and co-transfected with 1.8 µg of different luciferase-coupled promoter constructions described above and 0.2µg of β-galactosidase vector using JetPrime. Twenty-four hours later, cells were lysed in reporter lysis buffer (E1500, Promega, Charbonnieres-Les-Bains, France) then 20 µl of cells extracts were transferred to a 96-well plate and luminescence signal analyzed in a microplate reader (Varioskan). β-galactosidase activity analysis was performed to normalize promoter transfection efficiency by means of E200 kit (Promega) according to manufacturer conditions in Varioskan microplate reader. Luciferase signals were normalized by both ß-galactosidase activity and Bradford protein concentration measurements.

Animal studies

C57BL6 control (PK+) and *PRKN* gene Knockout male mice (PK-) [18] were housed with a 12:12 h light/dark cycle and were given free access to food and water. All experimental procedures were in accordance with the European Communities Council Directive of 24 November 1986 (86/609/EEC) and local French legislation.

PK+ and PK- randomized mice (9 months old) were intraperitonially injected with paraquat 10 mg/kg (36541, Sigma-Aldrich), each 3 days during 15 days using saline as control. Mice brains (N = 6 per group) were then recovered for further protein analysis. In a subset of experiments blood and perfused brains of PK+ and PK- (N = 6, 3-month-old) mice were collected for VPLEX analysis. In brief, the blood was recovered by incising the right atrium to allow exsanguination prior to PBS perfusion and brain recovery. Samples were transferred into clot-activator tubes and left at room temperature for 2 hours to allow coagulation. Tubes were then centrifuged at 10 000 × g for 20 minutes, and the supernatant (serum) was collected and stored at −80 °C until analysis. For a subset of mice, the *striatum* of PK+ and PK- randomized mice at different ages (3 and 9 months old) was microdissected for a posterior analysis of mRNA levels.

mRNA analysis (RT-qPCR)

RNA from cells or brains were extracted and treated with DNAse using RNeasy or RNeasy Plus Universal Mini kits respectively following manufacturer's instructions (Qiagen, Hilden, Germany). 4 µg of total RNA were reverse transcribed (A2791, GoScript Reverse Transcriptase, Promega) using Oligo-dT (, Promega) priming. Then, samples were subjected to real-time PCR by means of a Rotor-Gene 6000 apparatus (Qiagen), using the SYBR Green detection protocol. Gene-specific primers were designed with PrimerBlast (NCBI) or LabMaster (https://labmaster.streamlit.app/design_primer) then verified *in-silico* with UCSC *in-silico* PCR (UCSC). Gene-specific mRNA expression was normalized with mRNA expression of a house keeping gene: *GAPDH*).

Gene name	Forward (5' to 3')	Reverse (5' to 3')
PK (human)	AAAACCACCAAGCCCTGTC	TGCGGACACTTCATGTGC
iNOS (human)	CCACCTGACCTTGTGCTTGA	GGCGTACCACTTTAGCTCCA
GAPDH (human)	AGCCACATCGCTCAGACAC	GCCCAATACGACCAAATCC
iNos (mouse)	GTGACCATGGAGCATCCCAA	TCGAACTCCAATCTCGGTGC
Gapdh (mouse)	TGTCCGTCGTGGATCTGAC	CCTGCTTCACCACCTTCTTG

Immunofluorescence microscopy

HMC3 cells were plated on 18 mm coverslips previously coated with 0,05 mg/mL of poly-L-lysine for 2 hours at 37 °C. Then, cells were fixed with 4% paraformaldehyde for 30 min and permeabilized with 0,1 X Triton-X100 for 10 min. Nonspecific sites were blocked for 20 min with 5% BSA in PBS buffer containing 0,05% Tween 20. Each cover slip was incubated for 2 hours at room temperature with primary antibody (anti-PK (clone PRK8 Millipore MAB 5512), anti-human iNOS (E3W6B, Rabbit mAb Cell Signaling 20609)). A secondary donkey anti-mouse Alexa fluor-594 antibody or donkey anti-rabbit Alexa fluor-647 antibody (Molecular Probes DMS, 1:1000) were used to reveal the primary antibody and the nuclei were stained using DAPI (Molecular probes, 1:15000). GFP is endogenously expressed by pSBbi-Pur vector. Images were acquired either using an inverted laser scanning confocal microscope Leica TCS SP5 3X (Leica Microsystems, Nanterre, France) through a HC PL APO CS2 100X/1.4 oil immersion objective or with an epifluorescence microscope Axioplan2, Zeiss through a Plan-Apochromat 63×/1.40 oil DIC objective with immersion. Images were organized with OMERO, an open microscopy environment (OME). Final images were obtained after deconvolution using the Huygens Remote Manager version 3.7 (Scientific Volume Imaging, The Netherlands), using the CMLE algorithm, with SNR:45 and 40 iterations.

Multi-Plex (V-Plex)

Cytokines analysis in serum and mouse brain tissue was performed using the VPLEX Proinflammatory Panel 1 Mouse kit (MesoScale, Rockville, Maryland, USA), following the manufacturer's guidelines. In brief, to prepare the mouse brain samples, tissues were lysed (50-150 mg/sample) with 1 ml of 10 mM Tris buffer (pH 7.5) supplemented with a cocktail of protease inhibitors (P2714, Sigma-Aldrich) at 4 °C to prevent protein degradation. Samples are then mechanically ground using MagNALyser Green Beads in a MagNALyser (Roche Life Science, Bâle, Switzerland), after which they are incubated on ice for 30 minutes and centrifuged for 10 minutes at 14,000 rpm at 4 °C. Two hundred micrograms of protein are taken up in a final volume of 60 µL of dilution buffer provided by the VPLEX kit, and 50 µL are analyzed

according to the supplier's protocol. Meanwhile, the serum is diluted twice using the same diluent, and 50 µL are analyzed according to the supplier's protocol.

Electrophoretic Mobility Shift Assay (EMSA)

EMSA assays were performed using either nuclear extracts prepared from HMC3 control cells or overexpressing PK or recombinant PK cultured in 100-mm diameter dishes according to protocols of NE-PER™ Cytoplasmic and Nuclear Extraction Reagents (78833, Thermo Fischer).

Cold probes and 5' biotinylated probes were amplified by PCR (Forward primer: 5'-TCAGGCAAAGGCACCCCTG-3'; Reverse primer: 5'-CTTCATCACTGGCCACAGGCA-3') using PFU polymerase (M7745, Promega) and wild-type iNOS promoter cloned in pGL3-luciferase plasmid as a matrice and purified by agarose gel electrophoresis and gel extraction with Gel Extraction kit from Qiagen.

For EMSA assay using HMC3 cells as the source of PK, 10 µg of nuclear extracts were incubated in 10X binding buffer (100 mM Tris, 500 mM KCl, 10 mM DTT; pH:7.5), glycerol (final concentration 2.5 %) and poly (dI-dC) (final concentration 50 ng/µL) (all reagents from EMSA kit 20148, Thermo Scientific) at 21°C for 20 min with 20 fmol of distinct double stranded 5' biotin end-labeled oligonucleotides bearing or not the putative parkin consensus motif.

For the *in-vitro* EMSA assay, 200 ng of purified wild-type recombinant PK (23-048, Merck Millipore, Molsheim, France) were incubated in 10X binding buffer (100 mM Tris, 500 mM KCl, 10 mM DTT; pH:7.5) and glycerol (final concentration 2.5 %) (all reagents from EMSA kit 20148, Thermo Scientific) at 21°C for 20 min with 20 fmol of distinct double stranded 5'biotin end-labeled oligonucleotides bearing or not the putative parkin consensus motif.

Complexes are then resolved by electrophoresis on a 6% native polyacrylamide gel at 4°C, transferred to a positively charged nylon B membrane (77016, Thermo Scientific), crosslinked (UV-light cross-linker equipped with a 254 nm bulb) and revealed by means of streptavidin conjugated to horseradish peroxidase (HRP, 20148, Thermo Scientific) and a chemiluminescent substrate (20148, Thermo

Scientific). When indicated a 5 min pre-incubation with an excess (4 pmol) of unlabeled specific probes before adding the biotin-labeled probes was performed to confirm specific DNA-protein interaction.

In-silico promoter analysis

Human iNOS promoter and mouse iNos promoter were extracted using TFinder [19] from -2000/+2000 from TSS. Human genome: GRCh38, Mouse genome: GRCm39. Both promoters were aligned by EMBOSS Needle Pairwise Sequence Alignment. Prediction of parkin response element: PKRE on human iNOS promoter and mouse iNOS promoter was performed using Position Weight Matrix of PKRE created by the comparison of promoter sequences validated for PK binding by ChIP and EMSA. WebLogo, prediction of PKRE, and scores calculations were performed using TFinder. Alignment of conserved PKRE on human and mouse promoters was performed using Needlman-Wunsch from NCBI tools.

Statistical analysis

Statistical analysis was performed with GraphPad Prism software (San Diego, California USA). The choice of parametric versus nonparametric test was established after assessment of the normality test (D'Agostino-Pearson omnibus or Shapiro Normality test) to assure Gaussian distribution of values. Two groups of variables that have passed the normality test were analyzed by unpaired Student's t-test while two groups of variables that have not passed the normality test were analyzed by the Mann Whitney test. Grouped analysis of one or more groups was performed by two-way ANOVA followed by Tukey's multiple-com comparisons test. All tests are two-sided; the mean was defined as the center value and errors bars correspond to SEM. The number of samples, replication of experiments, post hoc tests and the P values (stars) are provided in results and figures legends. Outliers were removed by Graphad tool.

RESULTS

PK controls proliferation, phagocytosis and NO production

Since microgliosis, the activation and proliferation of microglia, concerns a key process of NIF [20], we have evaluated the contribution of PK in human and mouse microglial cells proliferation.

The real-time analysis of proliferation by means of XCELLigence technology demonstrates that PK overexpression **(Figure 1A,** N = 8, Student's t test, P<0.0001) triggers a drastic reduction of human microglial cells 3 (HMC3) cells proliferation (**Figure 1B,** N = 9). This impact of PK on HMC3 proliferation was evaluated by the analysis of two parameters; the slope of proliferation curves and the cells doubling time. **Figure 1C, D** (N = 9, Student's t test, P<0.0001) shows that PK overexpression leads to a significant reduction of HMC3 proliferation rate or an increase of its doubling time. It is important to note that we have only examined the impact of PK in basal conditions because the frequently used lipopolysaccharide (LPS) to prime inflammation does not modulate HCM3 proliferation. Next, to investigate whether changes in the distribution of cell cycle phases could account for the PK-related modulation of cell proliferation, we performed a flow cytometry analysis of HMC3 cells labelled with propidium iodide, a classic DNA intercalator. HMC3 cells overexpressing PK exhibited a significant decrease number of cells in the G1/G0 phase, an increase in the G2/M phase (**Figures 1E, F**, N = 9, Two-way ANOVA (Turkey), P<0.0001) and no modulation of the S phase. Since PK can modulate cyclins, via both its transcriptional and E3-ligase functions, [21-24] functionally linked to G1/S and G2/M phases control, we have examined its impact in the regulation of cyclins D and B protein levels. Both cyclins were not modulated by PK in HMC3 overexpressing cells (data not shown) suggesting that other cell cycle mediators are impacted by PK in microglial cells.

Next, we evaluated the effect of PK on the control of phagocytosis, another process related to microglia activation. Phagocytosis analysis by FACS approach shows that HMC3 cells that have internalized more than two beads exhibit a similar significant PK-induced reduction of phagocytic activity in both basal and LPS induced conditions **(Figure 1G,** N = 5, Two-way ANOVA**).**

The data set provided in **Figure 1** shows for the first time in a human microglial cell model, an anti-inflammatory effect of PK.

Likewise, the overexpression of PK (**Figure 2A**, N = 9, Student's t test) in a BV2 murine microglial cell line model slows down proliferation, as determined by slope (**Figure 2B, C** N = 9, Student's t test, $P<0.01$) and doubling time (**Figure 2B, D,** N = 9, Student's t test, $P<0.05$) measurements. The analysis of cell cycle reveals an increase in the G1/G0 phase, a decrease in the S phase and no modulation of the G2/M in the BV2 cell line (**Figure 2E, F,** N = 6, Two-way ANOVA (Turkey), $P<0.0001$). These results confirm the impact of PK in the downregulation of microglial proliferation in mice microglial cells and suggest that its impact to S phase may be cell-type-dependent.

Next, we have investigated the impact of PK in the regulation of a key mediator of pro-inflammatory response, nitric oxide (NO) [10, 25]. Since the levels of NO are under detection limits in HMC3 [26], we have examined the effect of PK overexpression in NO production in BV2 cells. **Figure 2G** (N = 6, Two-way ANOVA (Turkey), $P<0.01$, $P<0.0001$) shows that NO became detectable at approximately 9 hours post-stimulation, peaked at 16 hours, and gradually declined thereafter in EV-expressing cells. Notably, PK overexpression significantly reduced NO levels at the 16-hour peak, indicating a regulatory role for parkin in modulating NO production during microglial activation.

PK-iNOS functional cross-talk governs PK-associated control of neuroinflammation

The fact that PK controls NO levels and that PK is nitrosylated by a yet unknown mechanism led us to hypothesize that a bidirectional regulatory loop could link these proteins. To address this question, first, we have investigated if PK was implicated in the regulation of the enzyme responsible for NO production, iNOS. **Figure 3A, B** (N = 16, Two-way ANOVA, $P<0.01$, $P<0.0001$) shows that LPS treatment leads to an increase of iNOS protein levels in control (compare red bars in Fig. 3B) but not in PK overexpressing (compare blue bars in Fig. 3B) HMC3 cells. Importantly, PK overexpression triggers a significant decrease of iNOS levels in LPS conditions that allow a reliable detection of iNOS by immunohistochemical approach.

Second, to determine if iNOS was involved in PK S-nitrosylation, we used human HMC3 microglial cells stably overexpressing PK and engineered to express iNOS in a doxycycline-inducible manner. Using SNO-RAC purification, we demonstrate that PK is specifically nitrosylated upon iNOS induction

in the absence of any external inflammatory stimuli (**Figure 3C**). GAPDH (Glyceraldehyde-3-Phosphate Dehydrogenase), a known iNOS nitrosylation target, served as a positive control in our experimental setting, confirming the specificity and efficiency of the assay. This data establishes that PK impact to iNOS regulation concerns a mechanism of autoregulation of PK levels.

Parkin transcriptionally regulates iNOS by direct binding to its promoter

Next, we have investigated the mechanism by which PK could control iNOS levels. Since PK is a transcription factor, we have first investigated if PK could control *iNOS* mRNA levels. Analysis of *iNOS* mRNA levels (**Figure 4A** N = 16, Two-way ANOVA, $P<0.001$) shows a reduction of iNOS in both basal and LPS conditions suggesting a transcriptional regulation. Next, to determine whether this transcriptional control could occur directly, we have analyzed *in-silico* the promoter sequence of iNOS with TFINDER [19] to determine if it contained reliable PKRE (PK-responsive element). We generated a consensus (PWM) from experimentally validated PK binding sites (ChIP and EMSA) on target genes (*TP53, PSEN1, PSEN2, CCNA2 and CCNB1*) using Clustal Omega and TFinder (**Figure 4B**). This matrix enabled us to identify several PKREs sites in human promoter (±2000 bp from the transcription start site (TSS)) with a high relative score (**Figure 4C**). The choice of this site for functional validation was based on its strong conservation in the mouse promoter.

We then cloned different regions of the human *iNOS* promoter into a luciferase reporter gene vector, retaining the PKRE site (WT Prom) or deleting it (ΔPKRE), by site-directed mutagenesis (**Figure 4D**). Analysis of PK impact on wild type *iNOS* promoter activity (**Figure 4E**, N = 16, Two-way ANOVA (Turkey), $P<0.01$, $P<0.001$, $P<0.0001$) shows that PK overexpression triggers a significant reduction of *iNOS* promoter activity in basal and LPS induced conditions in HCM3 cells. Of note, as previously described in the literature, this promoter does not contain a functional NFKB site, explaining its insensitivity to LPS induction (**Figure 4E**). Interestingly, when we performed the same analysis with the human *iNOS* promoter deleted of PKRE (+1290), we observed a full abolishment of PK ability to repress *iNOS* promoter activity in basal and LPS conditions indicating that this pre-mapped PKRE was genuinely functional.

Next, to determine if PK regulation of *iNOS* promoter was direct, we performed an EMSA (electrophoretic mobility shift assay) using nuclear extracts from HMC3 cells overexpressing or not PK. **Figure 4F** shows that overexpressed PK interacts with the biotinylated probe containing PKRE and that this interaction is reversed by an excess of cold probe highlighting the specificity of the interaction. Finally, to rule out the involvement of other transcriptions factors in PK-mediated iNOS transcription control, we reproduced the EMSA using purified recombinant PK and confirmed a direct, specific interaction with the PKRE-containing probe (**Figure 4G**).

Endogenous PK invalidation a pro-inflammatory profile in mice brain and serum

To evaluate the effect of PK in the control of NIF *in-vivo*, we examined the cytokines profile in young adult wild-type (WT) and PK KO mice in either brain (**Figure 5A-H**) or serum (**Figure 6A-H**). The statistical analysis of the indicated detectable cytokines in mice brains show a significant increase in interleukin (IL)-10 (**Figure 5F**, N = 6, Mann Whitney test**, P<0.01**).

At the peripheral level, the investigation of the same cytokines in the serum of the same mice showed a significant increase in IL5 (**Figure 6C**, N = 8, Mann Whitney test, P<0.01) and IFNγ (**Figure 6F**, N = 10 WT and 12 KO PK, Mann Whitney test, P<0.001). These results suggest that the inflammatory profile is consistently but variably dysregulated in the absence of PK, at both the central and peripheral levels in basal conditions.

Paraquat treatment abolishes parkin-mediated regulation of iNOS

To examine the impact of PK in iNOS regulation in a sporadic PD *in vivo* model, we have chosen paraquat, an herbicide that, besides its well characterized neurotoxic effect [27], was shown to impact PK TF function via enhanced nitrosylation of PK [4].

Since the comparison of the impact of PK knockout in the *striatum* according to age only showed a regulation of *iNos* mRNA levels in aged mice (**Figure 7A**, N = 3-4, Welch's t test), we have explored the effect of paraquat in nine-month-old wild-type (WT) and knockout (KO) mice. **Figure 7B,C** (N = 6, Two-way ANOVA (Turkey) , P<0.0001) shows that KO PK mice have increased levels of iNOS

protein in basal conditions (compare black bars) corroborating the mRNA data showed in **Figure 7A**. Importantly, paraquat treatment fully prevents PK KO-linked up-regulation of iNOS (compare white bars) corroborating the impact on PK transcription factor in sporadic PD.

DISCUSSION

The physiopathology of PD is multifactorial and complex, and an increasing body of evidence pinpoints the implication of neuroinflammation in the etiology of the disease.

Typical pathological hallmarks of PD-affected brain involve the aggregation of α-synuclein within so-called Lewy bodies, alongside the progressive loss of dopaminergic neurons in the *substantia nigra pars compacta*. Besides, chronic neuroinflammatory processes, mainly mediated by glial cells and infiltrating immune cells, emerge as key facilitators of neuronal injury and disease progression.

Interestingly, several studies highlighted the contribution of mutations in genes associated with PD (linked to both autosomal dominant and recessive forms) in the control of NIF. Thus, mutations in LRRK2, PINK1, parkin, and DJ-1 affect neuroinflammatory processes [28, 29]. Of note the demonstration of the link between mitophagy dysfunction and robust inflammatory responses in glia via the liberation of DAMPS, highlighted the implication of parkin as a key molecular player involved in the control of neuroinflammation.

PK, is a recognized E3 ubiquitin ligase implicated in the regulation of mitochondrial quality control, that also plays a key role in the immune response. In particular, it controls mitophagy in cooperation with PINK1, thereby preventing the release of mitochondrial DAMPs that can activate inflammatory pathways [5, 6, 11]. However, we recently described a transcription factor function (TF) of PK [3], the implication of which in NIF has yet to be documented.

Most studies investigating the contribution of PK to NIF control have been performed using mouse cellular models. In this study, we examined the contribution of PK TF fuction in the control of NIF in a human cell line. Since NIF process is tightly linked to microglial response, firstly, we have assessed the effect of PK in the regulation of microglial functions, including microgliosis. The results shown in figure 1 demonstrates the ability of PK to reduce the proliferation of microglia in agreement with its anti-inflammatory properties mostly described in murine cells. Since several works have shown the impact of PK in the regulation of cyclins both via its E3-ligase and TF functions [21, 30, 31], to evidence the mechanisms by which PK could reduce the proliferation of microglial cells, we have examined the

influence of PK on cell cycle dynamics in both murine and human microglial cells. First, we confirmed the PK-mediated phenotype in murine BV2 cells that fully matches the one observed in human cells. Interestingly, our data shows that PK impacts cell cycle differently in both murine and human microglial cells. Thus, in human cells it impacts the G1/S and G2/M phases, while in murine cells, its anti-proliferative effect is mainly linked to a reduction of the number of cells in S phase. This apparently paradoxical data led us to determine if PK was involved in the regulations of cyclin D/E, A, B, that are key modulators of phases G1/S, S and G2/M, respectively. Our results show no modulation of cyclins in microglial cells. Since various studies have reported on the effect of PK on the regulation of cyclins in glioblastoma and HELA cells, the impact of PK on cell cycle control could well be dependent of cellular context [21, 30-32]. These results also suggest that other cell cycle players may be involved in PK-mediated control of proliferation. Notably it has been shown that PK induces G2/M cell cycle arrest in TNFα-treated HeLa cells by means of CDC2 inactivation [32]. Additional studies will be necessary to determine which PK transcriptional targets linked to cell cycle are involved in the control of microglial proliferation.

Since PK nitrosylation impacts both its E3-ligase [16] and TF functions [4], the evaluation of PK as a putative modulator of NO production was of interest. NO is a signal molecule that plays a crucial role in a variety of signal transduction pathways contributing to the homeostasis of vascular, respiratory, immune, muscular, and nervous systems. In addition, NO can act, depending on the redox state and/or its concentrations as a neurotoxin or as a neuroprotective factor. Multiple studies have demonstrated the implication of NO in PD [33], however, the molecular mechanisms underlying NO contribution to NIF in microglial cells is not fully established.

We show in Figure 2G that PK reduces NO production in BV2 cells in a time dependent manner in LPS stimulated conditions. This data suggests the implication of a tailored mechanism of regulation of NO production reminiscent of bell-shaped gene transcription regulation. These results coupled with the *in-silico* identification of conserved PKRE in the mouse and human iNOS promoters led us to examine the contribution of PK TF function in the regulation of iNOS, the enzyme involved in NO synthesis.

Figure 3 clearly demonstrates, using electrophoretic mobility shift assays (EMSAs), that PK regulates iNOS transcription via its direct binding to the TFINDER pre-mapped PKRE in +1290 position to TSS. It is important to note that even if the regulation of genes involved in NIF by PK has been reported [8], iNOS is to the best of our knowledge, the first PK direct transcriptional target involved in NIF. This discovery opens extremely interesting new perspectives on the involvement of PK in diseases related to neuroinflammation. Of note, the direct transcriptional regulation of iNOS by PK demonstrated by EMSA does not preclude the implication of its E3-ligase activity. Several of its validated transcriptional targets are also regulated at the post-transcriptional level via its E3-ligase activity, notably cyclin B and p53 [21, 34]. It is also interesting to note that the nitrosylation process is increased in PD [35] and that nitrosylation may abolish PK TF function by altering its subcellular localization [4]. Thus, it is likely that PK mislocalization due to its nitrosylation (aging, drugs) favors the chronic accumulation of toxic NO and neuroinflammation development in PD.

In agreement with this hypothesis, we show that iNOS levels are increased in PK KO mice brain and that this regulation is abolished in paraquat-treated mice. We show that iNOS is implicated in PK nitrosylation and that PK controls its own nitrosylation via the transcriptional regulation of iNOS. Moreover, since other mechanisms of PK regulation in inflammatory conditions have been described, it will be interesting to establish if this functional cross-talk between PK and iNOS is impacted according to the inflammatory context.

Finally, we have explored the effect of endogenous PK depletion in the control of the inflammatory response at central and periphery levels. Thus, we show a significant increase of IL10 in mice brain from PK KO mice. The increase of IL10, an anti-inflammatory associated interleukin in PK KO mice brains is somehow unexpected, but corroborated by several studies showing its increase in traumatic brain injury [36], Alzheimer [37] and Parkinson disease [38, 39]. Moreover, the examination of IL10 therapeutic impact *in-vivo* has unraveled its deleterious effect on mice model of synucleinopathy [40]. These results suggest that the level of IL10 should be further examined *in-vivo* and that multiple elements should be taken in consideration including the cell source (neurons, microglia astrocytes) and age. The upregulation of IL10 observed in young adult KO PK may be a consequence of a compensatory

mechanism aiming at circumscribing the exacerbated NIF response linked to the absence of endogenous PK.

The analysis of the same panel of cytokines at periphery levels indicates a significant increase of IFNγ and IL5 and decrease of IL1β. These modulations clearly reflect a deregulation of cytokines equilibrium between anti-inflammatory and pro-inflammatory. These results indicate that there is no concordance between the cytokines regulated by PK in the brain and the periphery suggesting that PK-modulated cytokines may either contribute to or result from PK-mediated control of neuroinflammation NIF. These results are also in agreement with the beneficial anti-inflammatory role of PK described so far since IL5 and IFNγ are well as pro-inflammatory factors. Of interest an increase of IFNγ has been evidenced in the plasma of PD-treated and -untreated patients [41]. It is worth noting that our study is the first demonstration of IL5 modulation in a PD context. IL5 is a cytokine primarily implicated in the physiopathology of atopic diseases, notably via the specific control of eosinophils production. Its role in the pathophysiology of PD remains to be established but its strong implication in asthma [42] reinforces the link of PK to inflammatory chronic diseases.

Previous and more recent studies have established that PK plays a wider role than just regulating mitochondrial homeostasis, intervening in various cellular processes such as inflammation, cell cycle and transcription regulation. Our study is the first demonstration that PK can directly control the transcription of the iNOS gene in glial cells. This adds to the body of knowledge documenting the functional pleiotropy of PK and the involvement of its TF function in unexpected cellular processes besides its well documented canonical role in the control of mitoophagy. Hopefully, this should open several promising avenues envisioning the role of PK in neuroinflammation and neurodegeneration.

DATA AND MATERIALS AVAILABILITY: All data are available in the main text or the supplementary materials.

ACKNOWLEDGEMENTS

We would like to thank Dr Inger Lauritzen for the administration of Paraquat in mice.

AUTHOR CONTRIBUTION

Conceptualization: CAC; Investigation: JM, ED, AB, CB, LRdS, MEB, HLB; Funding acquisition: CAC, LRB, FC; Project administration: CAC; Supervision CAC, ED; Writing-original draft: CAC; Writing review and editing: all authors.

FUNDING

This work was supported by “Conseil Général des Alpes Maritimes” and the Foundation Claude Pompidou. This work has been developed and supported through the LABEX (excellence laboratory, program investment for the future) DISTALZ (Development of Innovative Strategies for a Transdisciplinary approach to ALZheimer disease). JM was supported by “France Parkinson” foundation. MEB and LRB were supported by grants from São Paulo Research Foundation (FAPESP, Brazil).

COMPETING INTERESTS: The authors declare no conflict of interest.

ETHICS APPROVAL AND CONSENT TO PARTIPATE

This study was conducted in compliance with the principles of the Declaration of Helsinki. Informed consent was obtained from all the subjects. Animal experimental procedures were carried out in accordance with the Directive 2010/63/EU directive 2010/63/EU of the European parliament and of the council of 22 September 2010 after approval of the use of animals for experimental purposes by the local French Ethics.

REFERENCES

[1] G. Gelders, V. Baekelandt, A. Van der Perren, Linking Neuroinflammation and Neurodegeneration in Parkinson's Disease, J Immunol Res, 2018 (2018) 4784268.

[2] O. Corti, S. Lesage, A. Brice, What genetics tells us about the causes and mechanisms of Parkinson's disease, Physiol Rev, 91 (2011) 1161-1218.

[3] C. da Costa, C. Sunyach, E. Giaime, A. West, O. Corti, A. Brice, S. Safe, P. Abou-Sleiman, N. Wood, H. Takahashi, M. Goldberg, J. Shen, F.d.r. Checler, Transcriptional repression of p53 by parkin and impairment by mutations associated with autosomal recessive juvenile Parkinson's disease, Nature Cell Biology, 11 (2009) 1370-1375.

[4] C.R. Sunico, T. Nakamura, E. Rockenstein, M. Mante, A. Adame, S.F. Chan, T.F. Newmeyer, E. Masliah, N. Nakanishi, S.A. Lipton, S-Nitrosylation of parkin as a novel regulator of p53-mediated neuronal cell death in sporadic Parkinson's disease, Mol Neurodegener, 8 (2013) 29.

[5] L.E. Newman, G.S. Shadel, Pink1/Parkin link inflammation, mitochondrial stress, and neurodegeneration, The Journal of Cell Biology, 217 (2018) 3327-3329 %U https://rupress.org/jcb/article/3217/3310/3327/120257/Pink120251Parkin-link-inflammation-mitochondrial-stress.

[6] S.L. Pereira, D. Grossmann, S. Delcambre, A. Hermann, A. Grünewald, Novel insights into Parkin-mediated mitochondrial dysfunction and neuroinflammation in Parkinson's disease, Current Opinion in Neurobiology, 80 (2023) 102720 %U https://www.sciencedirect.com/science/article/pii/S0959438823000454.

[7] N. Panicker, T.-I. Kam, H. Wang, S. Neifert, S.-C. Chou, M. Kumar, S. Brahmachari, A. Jhaldiyal, J.T. Hinkle, F. Akkentli, X. Mao, E. Xu, S.S. Karuppagounder, E.T. Hsu, S.-U. Kang, O. Pletnikova, J. Troncoso, V.L. Dawson, T.M. Dawson, Neuronal NLRP3 is a parkin substrate that drives neurodegeneration in Parkinson’s disease, Neuron, 110 (2022) 2422-2437.e2429 %U https://linkinghub.elsevier.com/retrieve/pii/S0896627322004500.

[8] F. Mouton-Liger, T. Rosazza, J. Sepulveda-Diaz, A. Ieang, S.M. Hassoun, E. Claire, G. Mangone, A. Brice, P.P. Michel, J.C. Corvol, O. Corti, Parkin deficiency modulates NLRP3 inflammasome activation by attenuating an A20-dependent negative feedback loop, Glia, 66 (2018) 1736-1751.

[9] T.C. Frank-Cannon, T. Tran, K.A. Ruhn, T.N. Martinez, J. Hong, M. Marvin, M. Hartley, I. Trevino, D.E. O'Brien, B. Casey, M.S. Goldberg, M.G. Tansey, Parkin Deficiency Increases Vulnerability to Inflammation-Related Nigral Degeneration, Journal of Neuroscience, 28 (2008) 10825-10834 %U http://www.jneurosci.org/cgi/doi/10810.11523/JNEUROSCI.13001-10808.12008.

[10] T.A. Tran, A.D. Nguyen, J. Chang, M.S. Goldberg, J.K. Lee, M.G. Tansey, Lipopolysaccharide and tumor necrosis factor regulate Parkin expression via nuclear factor-kappa B, PLoS One, 6 (2011) e23660.

[11] D.A. Sliter, J. Martinez, L. Hao, X. Chen, N. Sun, T.D. Fischer, J.L. Burman, Y. Li, Z. Zhang, D.P. Narendra, H. Cai, M. Borsche, C. Klein, R.J. Youle, Parkin and PINK1 mitigate STING-induced inflammation, Nature, 561 (2018) 258-262 %U http://www.nature.com/articles/s41586-41018-40448-41589.

[12] Y.Q. Yan, R. Zheng, Y. Liu, Y. Ruan, Z.H. Lin, N.J. Xue, Y. Chen, B.R. Zhang, J.L. Pu, Parkin regulates microglial NLRP3 and represses neurodegeneration in Parkinson's disease, Aging Cell, 22 (2023) e13834 %U https://www.ncbi.nlm.nih.gov/pmc/articles/PMC10265164/.

[13] I.H. Henn, L. Bouman, J.S. Schlehe, A. Schlierf, J.E. Schramm, E. Wegener, K. Nakaso, C. Culmsee, B. Berninger, D. Krappmann, J. Tatzelt, K.F. Winklhofer, Parkin mediates neuroprotection through activation of IkappaB kinase/nuclear factor-kappaB signaling, J Neurosci, 27 (2007) 1868-1878.

[14] D. Sha, L.-S. Chin, L. Li, Phosphorylation of parkin by Parkinson disease-linked kinase PINK1 activates parkin E3 ligase function and NF-κB signaling, Human Molecular Genetics, 19 (2010) 352-363 %U https://doi.org/310.1093/hmg/ddp1501.

[15] Y. Wang, B. Shan, Y. Liang, H. Wei, J. Yuan, Parkin regulates NF-κB by mediating site-specific ubiquitination of RIPK1, Cell Death & Disease, 9 (2018) 732 %* 2018 The Author(s) %U https://www.nature.com/articles/s41419-41018-40770-z.

[16] K.K. Chung, B. Thomas, X. Li, O. Pletnikova, J.C. Troncoso, L. Marsh, V.L. Dawson, T.M. Dawson, S-nitrosylation of parkin regulates ubiquitination and compromises parkin's protective function, Science, 304 (2004) 1328-1331.

[17] P. Seth, R.T. Premont, J.S. Stamler, An optimized protocol for isolation of S-nitrosylated proteins from C. elegans, STAR Protocols, 2 (2021) 100547 %U https://linkinghub.elsevier.com/retrieve/pii/S2666166721002549.

[18] J.M. Itier, P. Ibanez, M.A. Mena, N. Abbas, C. Cohen-Salmon, G.A. Bohme, M. Laville, J. Pratt, O. Corti, L. Pradier, G. Ret, C. Joubert, M. Periquet, F. Araujo, J. Negroni, M.J. Casarejos, S. Canals, R. Solano, A. Serrano, E. Gallego, M. Sanchez, P. Denefle, J. Benavides, G. Tremp, T.A. Rooney, A. Brice, J. Garcia de Yebenes, Parkin gene inactivation alters behaviour and dopamine neurotransmission in the mouse, Hum Mol Genet, 12 (2003) 2277-2291.

[19] J. Minniti, F. Checler, E. Duplan, C. Alves da Costa, TFinder: A Python Web Tool for Predicting Transcription Factor Binding Sites, Journal of Molecular Biology, 437 (2025) 168921 %* Versement au domaine public en vertu de CC168920 168921.168920 Universel. %U https://linkinghub.elsevier.com/retrieve/pii/S0022283624005515.

[20] F. Aloisi, Immune function of microglia, Glia, 36 (2001) 165-179 %* Copyright © 2001 Wiley-Liss, Inc. %U https://onlinelibrary.wiley.com/doi/abs/2010.1002/glia.1106.

[21] L. Rouland, E. Duplan, L. Ramos Dos Santos, A. Bernardin, K.S. Katula, G. Manfioletti, A. Idbaih, F. Checler, C. Alves da Costa, Therapeutic potential of parkin as a tumor suppressor via transcriptional control of cyclins in glioblastoma cell and animal models, Theranostics, 11 (2021) 10047-10063.

[22] Y. Gong, T.I. Zack, L.G. Morris, K. Lin, E. Hukkelhoven, R. Raheja, I.L. Tan, S. Turcan, S. Veeriah, S. Meng, A. Viale, S.E. Schumacher, P. Palmedo, R. Beroukhim, T.A. Chan, Pan-cancer genetic analysis identifies PARK2 as a master regulator of G1/S cyclins, Nat Genet, 46 (2014) 588-594.

[23] M. Karpurapu, D. Wang, N.K. Singh, Q. Li, G.N. Rao, NFATc1 Targets Cyclin A in the Regulation of Vascular Smooth Muscle Cell Multiplication during Restenosis, Journal of Biological Chemistry, 283 (2008) 26577-26590 %U https://linkinghub.elsevier.com/retrieve/pii/S0021925820524022.

[24] M. Karpurapu, D. Wang, D. Van Quyen, T.-K. Kim, V. Kundumani-Sridharan, S. Pulusani, G.N. Rao, Cyclin D1 Is a Bona Fide Target Gene of NFATc1 and Is Sufficient in the Mediation of Injury-induced Vascular Wall Remodeling, Journal of Biological Chemistry, 285 (2010) 3510-3523 %U https://linkinghub.elsevier.com/retrieve/pii/S0021925820648451.

[25] T.C. Frank-Cannon, T. Tran, K.A. Ruhn, T.N. Martinez, J. Hong, M. Marvin, M. Hartley, I. Trevino, D.E. O'Brien, B. Casey, M.S. Goldberg, M.G. Tansey, Parkin deficiency increases vulnerability to inflammation-related nigral degeneration, J Neurosci, 28 (2008) 10825-10834.

[26] Z. Woolf, T.J. Stevenson, K. Lee, B. Highet, J. Macapagal Foliaki, R. Ratiu, J. Rustenhoven, J. Correia, P. Schweder, P. Heppner, M. Weinert, N. Coppieters, T. Park, J. Montgomery, A.M. Smith, M. Dragunow, In vitro models of microglia: a comparative study, Scientific Reports, 15 (2025) 15621 %U https://www.nature.com/articles/s41598-15025-99867-z.

[27] P. Sharma, P. Mittal, Paraquat (herbicide) as a cause of Parkinson's Disease, Parkinsonism Relat Disord, 119 (2024) 105932.

[28] I. Chandel, S. Kumari, K. Bagri, A. Bhatia, R. Deshmukh, Parkinson's disease: genetics and neuroinflammatory insights, Inflammopharmacology, (2025).

[29] C. Castillo-Rangel, G. Marin, K.A. Hernandez-Contreras, M.M. Vichi-Ramirez, C. Zarate-Calderon, O. Torres-Pineda, D.L. Diaz-Chiguer, D. De la Mora Gonzalez, E. Gomez Apo, J.A. Teco-Cortes, F.M. Santos-Paez, M.L.A. Coello-Torres, M. Baldoncini, G. Reyes Soto, G.E. Aranda-Abreu,

L.I. Garcia, Neuroinflammation in Parkinson's Disease: From Gene to Clinic: A Systematic Review, Int J Mol Sci, 24 (2023).

[30] C.W. Yeo, F.S. Ng, C. Chai, J.M. Tan, G.R. Koh, Y.K. Chong, L.W. Koh, C.S. Foong, E. Sandanaraj, J.D. Holbrook, B.T. Ang, R. Takahashi, C. Tang, K.L. Lim, Parkin pathway activation mitigates glioma cell proliferation and predicts patient survival, Cancer Res, 72 (2012) 2543-2553.

[31] S. Veeriah, B. Taylor, S. Meng, F. Fang, E. Yilmaz, I. Vivanco, M. Janakiraman, N. Schultz, A. Hanrahan, W. Pao, M. Ladanyi, C. Sander, A. Heguy, E. Holland, P. Paty, P. Mischel, L. Liau, T. Cloughesy, I. Mellinghoff, D. Solit, T. Chan, Somatic mutations of the Parkinson's disease-associated gene PARK2 in glioblastoma and other human malignancies, Nature genetics, 42 (2010) 77-82.

[32] M.H. Lee, Y. Cho, B.C. Jung, S.H. Kim, Y.W. Kang, C.H. Pan, K.J. Rhee, Y.S. Kim, Parkin induces G2/M cell cycle arrest in TNF-alpha-treated HeLa cells, Biochem Biophys Res Commun, 464 (2015) 63-69.

[33] F.J. Jimenez-Jimenez, H. Alonso-Navarro, M.T. Herrero, E. Garcia-Martin, J.A. Agundez, An Update on the Role of Nitric Oxide in the Neurodegenerative Processes of Parkinson's Disease, Curr Med Chem, 23 (2016) 2666-2679.

[34] Y.Y. Jung, D.J. Son, H.L. Lee, D.H. Kim, M.J. Song, Y.W. Ham, Y. Kim, S.B. Han, M.H. Park, J.T. Hong, Loss of Parkin reduces inflammatory arthritis by inhibiting p53 degradation, Redox Biol, 12 (2017) 666-673.

[35] M.G. Stykel, S.D. Ryan, Nitrosative stress in Parkinson's disease, NPJ Parkinsons Dis, 8 (2022) 104.

[36] K. Kamm, W. Vanderkolk, C. Lawrence, M. Jonker, A.T. Davis, The effect of traumatic brain injury upon the concentration and expression of interleukin-1beta and interleukin-10 in the rat, J Trauma, 60 (2006) 152-157.

[37] J. Apelt, R. Schliebs, Beta-amyloid-induced glial expression of both pro- and anti-inflammatory cytokines in cerebral cortex of aged transgenic Tg2576 mice with Alzheimer plaque pathology, Brain Res, 894 (2001) 21-30.

[38] M. Rentzos, C. Nikolaou, E. Andreadou, G.P. Paraskevas, A. Rombos, M. Zoga, A. Tsoutsou, F. Boufidou, E. Kapaki, D. Vassilopoulos, Circulating interleukin-10 and interleukin-12 in Parkinson's disease, Acta Neurol Scand, 119 (2009) 332-337.

[39] X.Y. Qin, S.P. Zhang, C. Cao, Y.P. Loh, Y. Cheng, Aberrations in Peripheral Inflammatory Cytokine Levels in Parkinson Disease: A Systematic Review and Meta-analysis, JAMA Neurol, 73 (2016) 1316-1324.

[40] S.G. Cockey, K.N. McFarland, E.J. Koller, M.M.T. Brooks, E. Gonzalez De La Cruz, P.E. Cruz, C. Ceballos-Diaz, A.M. Rosario, Y.R. Levites, D.R. Borchelt, T.E. Golde, B.I. Giasson, P. Chakrabarty, Il-10 signaling reduces survival in mouse models of synucleinopathy, NPJ Parkinsons Dis, 7 (2021) 30.

[41] N. Kustrimovic, C. Comi, L. Magistrelli, E. Rasini, M. Legnaro, R. Bombelli, I. Aleksic, F. Blandini, B. Minafra, G. Riboldazzi, A. Sturchio, M. Mauri, G. Bono, F. Marino, M. Cosentino, Parkinson's disease patients have a complex phenotypic and functional Th1 bias: cross-sectional studies of CD4+ Th1/Th2/T17 and Treg in drug-naive and drug-treated patients, J Neuroinflammation, 15 (2018) 205.

[42] M. Dougan, G. Dranoff, S.K. Dougan, GM-CSF, IL-3, and IL-5 Family of Cytokines: Regulators of Inflammation, Immunity, 50 (2019) 796-811.

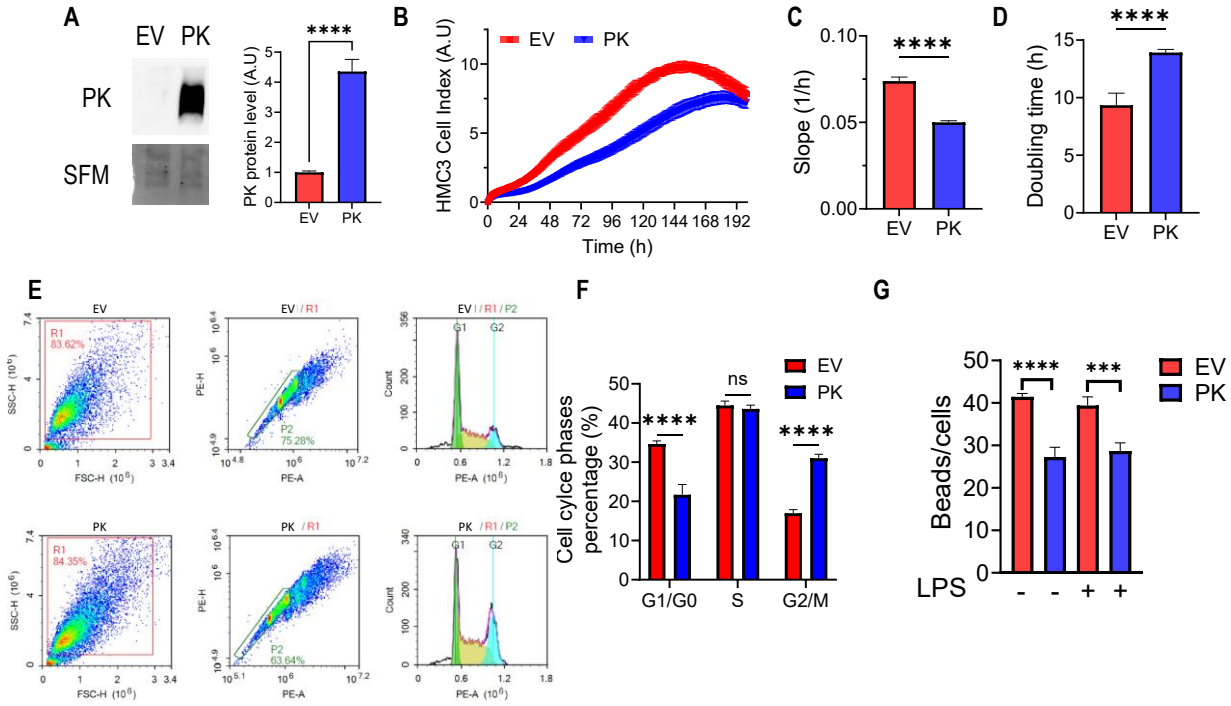


Figure 1: Parkin regulates proliferation and phagocytosis in HMC3 cells.

(A-G) HMC3 stably expressing empty pSBbi-Pur (EV, red) or wild type PK pSBbi-Pur-Parkin (PK, blue). **(A)** Western blot and quantification of PK expression normalized by total proteins quantity (Stain Free Membrane, SFM, N = 8 Student's t test). **(B, C, D)** illustrate the effect of PK overexpression on cellular proliferation of HMC3 cells assessed by impedance-based label free approach. (**B)** representation of proliferation curves. (**C)** Quantification analysis of the slopes, (N = 9 Student's t test). (**D)** Quantification analysis of doubling time (N = 9, Student's t test). Bars correspond to the means +/- SEM of 3 independent experiments performed in triplicates. **(E, F)** Effect of PK overexpression on cellular proliferation of HMC3 cells assessed by FACS approach. (**E**) representative images of gating procedure and **(F)** quantification of the percentage of cells in each phase of the cell cycle (G0/G1, S, G2/M, N = 9 Two-way ANOVA). Bars correspond to the means +/- SEM of 3 independent experiments performed in triplicates. Panel **G** (N = 5 Two-way ANOVA**)** illustrate the effect of PK overexpression on phagocytosis activity (% of cells that have internalized at least 2 beads) in basal condition and under LPS stress (1 µg/mL overnight) by FACS approach. Bars correspond to the means +/- SEM of 2 independent experiments performed in triplicates. *** $P < 0.001$; **** $P < 0.0001$, ns, non-significant.

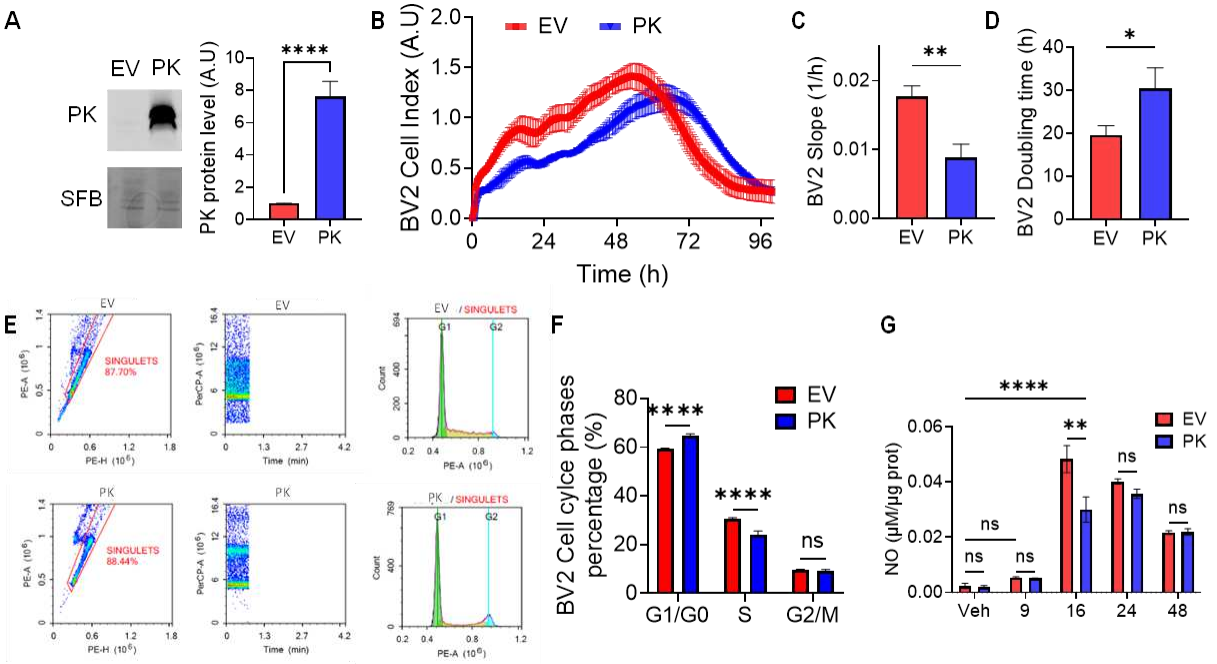


Figure 2: Parkin overexpression reduces proliferation and NO production in BV2 cells.

(A-G) BV2 stably expressing empty pSBbi-Pur (EV, red) or wild type PK pSBbi-Pur-Parkin (PK, blue). **(A)** Western blot and quantification analysis (normalized by total proteins quantity with Stain Free Membrane, SFM, N = 8 Student's t test) of PK expression in BV2. **(B, C, D)** Effect of PK overexpression on cellular proliferation of BV2 assessed by impedance-based label free approach. **(B)** representation of proliferation curves. **(C)** Quantification analysis of the slopes, N = 9 Student's t test). **(D,** N = 9, Kolmogorov-Smirnov**)** Quantification analysis of doubling time. Bars correspond to the means +/- SEM of 3 independent experiments performed in triplicates. **(E, F)** Illustrate the effect of PK overexpression on cellular proliferation of BV2 assessed by FACS approach. **(E)** Representative images of gating procedure. **(F)** Quantification of the percentage of cells in each phase of the cell cycle (G0/G1, S, G2/M, N = 6 Two-way ANOVA). Bars correspond to the means +/- SEM of 2 independent experiments performed in triplicates. **(G)** Kinetic of nitric oxide production under LPS stress (1 µg/m, N = 6 One-way ANOVA). Bars correspond to the means +/- SEM of 3 independent experiments performed in duplicate. * $P < 0.05$; ** $P < 0.01$ and **** $P < 0.000$, ns, non-significant.

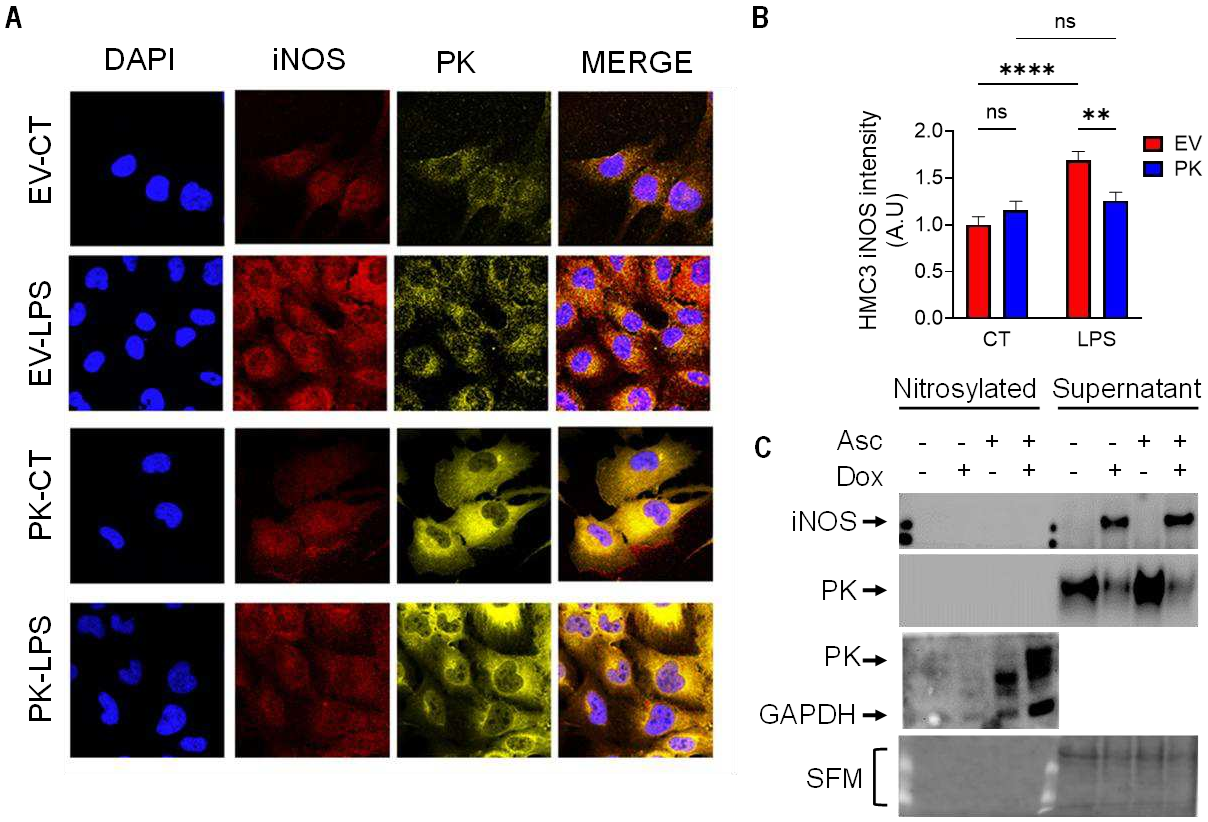
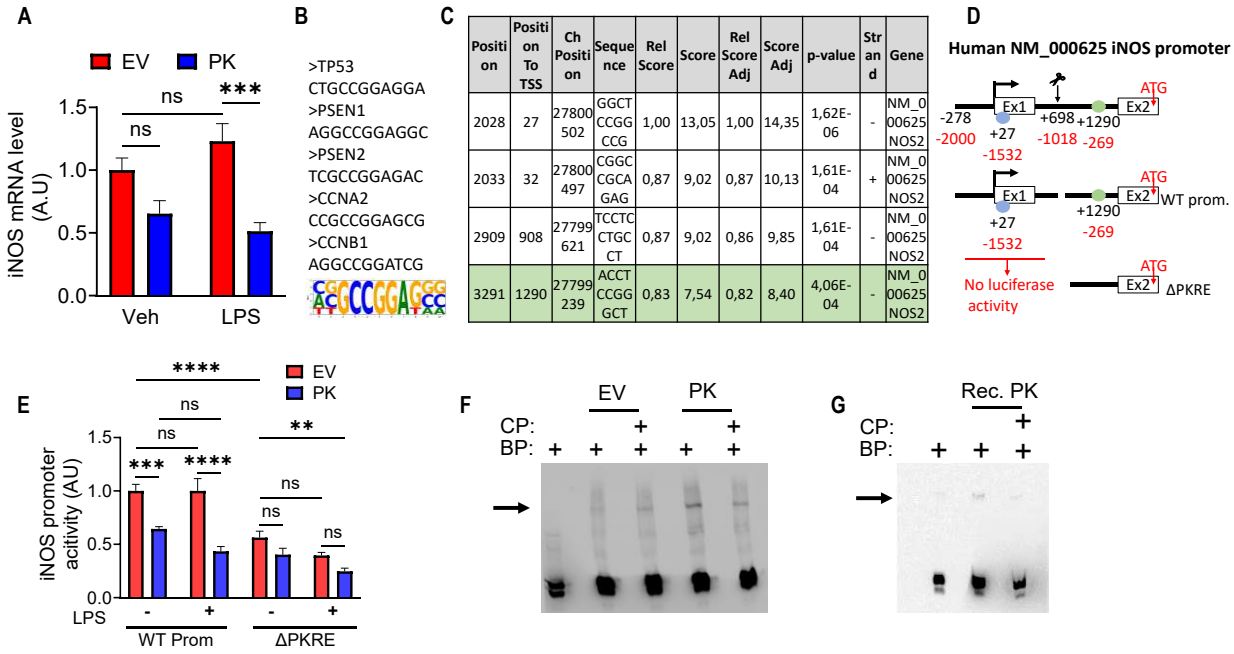


Figure 3: Parkin and iNOS functional cross-talk in HMC3.

(A, B) HMC3 stably expressing empty pSBbi-Pur (EV, red) or wild type PK pSBbi-Pur-Parkin (PK, blue. **(A, B)** Impact of PK on iNOS protein expression in basal (CT) and LPS conditions (24 hours at 1 µg/mL) analyzed by immunofluorescence microscopy. (**A**) Representative images of iNOS labeling quantified in **(B,** N = 16, Two-way ANOVA**)** as described in Materials and Methods. Bars correspond to the means +/- SEM of 4 independent experiments performed in quadruplicate. ** $P < 0.01$; *** $P < 0.001$ and, ns: non-significant. **(C)** Analysis of PK nitrosylation by iNOS in HMC3 stably expressing wild type PK pSBbi-Pur-Parkin and inducible iNOS by doxycycline pSBTet-Pur-iNOS. Western blot of nitrosylated protein captured by SNO-RAC approach as described in Materials and Methods. Data obtained in absence and presence of ascorbate (Asc) that allows binding of nitrosylated proteins to beads. Induction of iNOS was achieved by a treatment with doxycycline (Dox, 1 µM overnight). Representative blots of iNOS (to demonstrate its induction), PK (1) to show PK overexpression and PK (2) to show PK and GAPDH nitrosylation after cropping of supernatant samples to allow the reblot of (PK1, see Methods). Stain free membranes (SFM) are provided to show protein load.



759

760 **Figure 4:** Parkin regulates and interacts with endogenous iNOS promoter *in vitro* and in HMC3 cells.
761 **(A,** N = 16, Two-way ANOVA) Impact of PK to iNOS mRNA levels in basal and LPS conditions (24
762 hours at 1 µg/mL) by RT-qPCR. **(A)** Bars correspond to the means +/- SEM of 4 independent
763 experiments performed in quadruplicate. *** $p < 0.001$ and ns: non-significant. **(B)** Reference FASTA
764 sequence of PK targets (TP53, PSEN1, PSEN2, CCNA2 and CCNAB2) validated by ChIP and EMSA
765 used to generate Position Weight Matrix (PWM) of the PK Recognition Site (PKRE) and associated
766 WebLogo. **(C)** Prediction analysis of PK binding sites of the human and mouse iNos promoters (Human
767 genome: GRCh38, Mouse genome: GRCm39) with TFINDER. **(D)** Representative schematic
768 representation of human iNOS promoter. Blue circles correspond to +27 and +32 (from TSS) PKREs
769 but this promotor region didn't yield luciferase (data not show). Green circle corresponds to the + 1290
770 (from TSS) PKRE that is conserved (+ 1101, from TSS) on the mouse wild-type promoter (WT prom).
771 Deletion of + 1290 (from TSS) PKRE is labeled in red on alignment B, promoter called ΔPKRE. **(E) (**N
772 = 16, Two-way ANOVA**)** Wild-type and PKRE deleted iNOS promoter activity measurement in HMC3
773 stably expressing empty pSBbi-Pur (EV, red) or wild type PK pSBbi-Pur-Parkin (PK, blue) in control
774 and LPS conditions (1 µg/mL, 24 h). Bars correspond to the means +/- SEM of 4 independent
775 experiments performed in quadruplicates. ** $P < 0.01$; *** $P < 0.001$, **** $p < 0.0001$ and ns: non-

776 significant. **(F)** Electrophoretic mobility shift assay (EMSA) of nuclear extract (NE) of HMC3 cells
777 over-expressing human wild-type PK (PK) or empty vector (EV) incubated with biotinylated probes
778 (BP) with or without excess of cold probes (CP) including validated PKRE. **(G)** EMSA analysis of the
779 interaction of recombinant PK incubated with biotinylated probes (BP) with or without excess of cold
780 probes (CP) including validated PKRE.

781

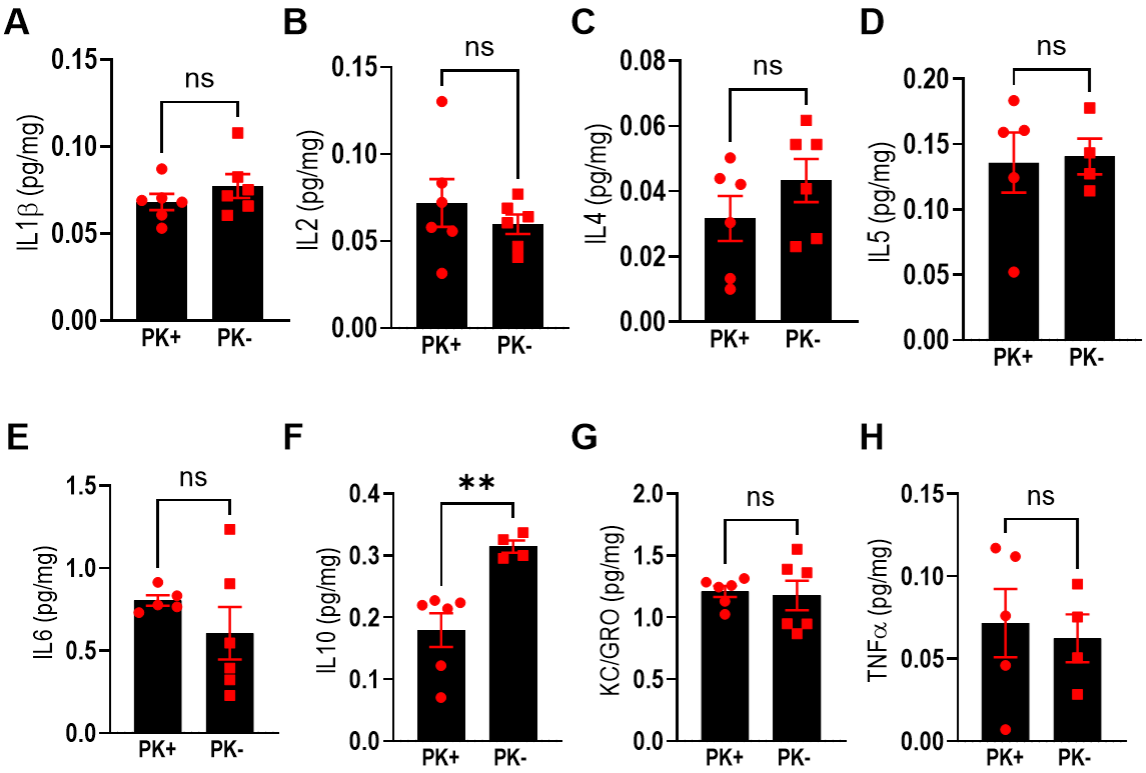


Figure 5: Impact of PK on cytokine levels in mice brain.

(A-H) VPLEX analysis of proinflammatory cytokines in the brain of 3 months-aged wild-type (PK+) and KO (PK-) mice. Panels A-H (Mann Whitney test) show the analysis of IL1β (**A**, N = 6), IL2 (**B**, N = 6), IL4 (**C**, N = 6), IL5 (**E**, N = 6), IL6 (**E**, N = 6), IL10 (**F**, N = 6), KC/GRO (**G**, N = 6), TNFα (**H**, N = 6). Bars correspond to the means +/- SEM. ** $p < 0.01$, ns: non-significant.

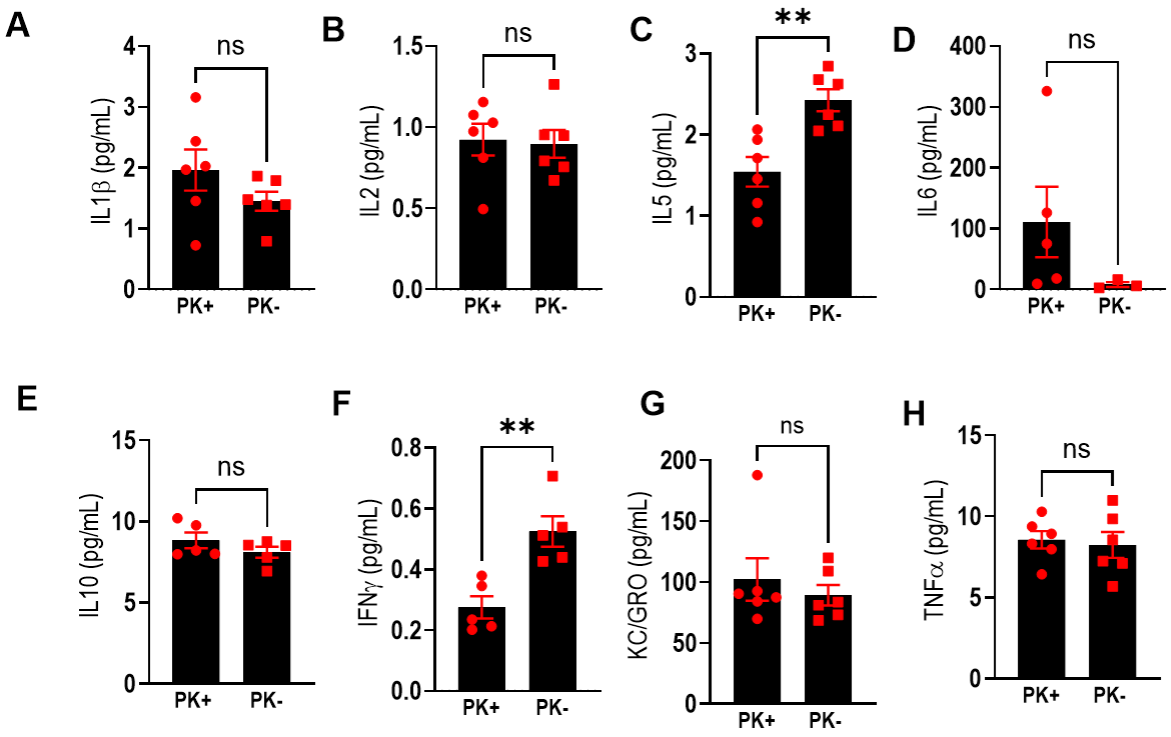


Figure 6: Impact of PK in peripheral cytokine regulation.

(A-H) VPLEX analysis of proinflammatory cytokines in the serum recovered from of 3 months-aged wild-type (PK+) and KO (PK-) mice. Panels **A-H** (Mann Whitney test) show the analysis of IL1β (**A**, N = 14 WT and 10 KO PK), IL2 (**B**, N = 6), IL5 (**C**, N = 8), IL6 (**D**, N = 7 WT and 6 KO PK), IL10 (**E**, N = 13), IFNγ (**F**, N=10 WT and 12 KO PK), KC/GRO (**G**, N = 13), TNFα (**H**, N = 14 WT and 13 KO PK). Bars correspond to the means +/- SEM. ** $p < 0.01$, ns: non-significant.

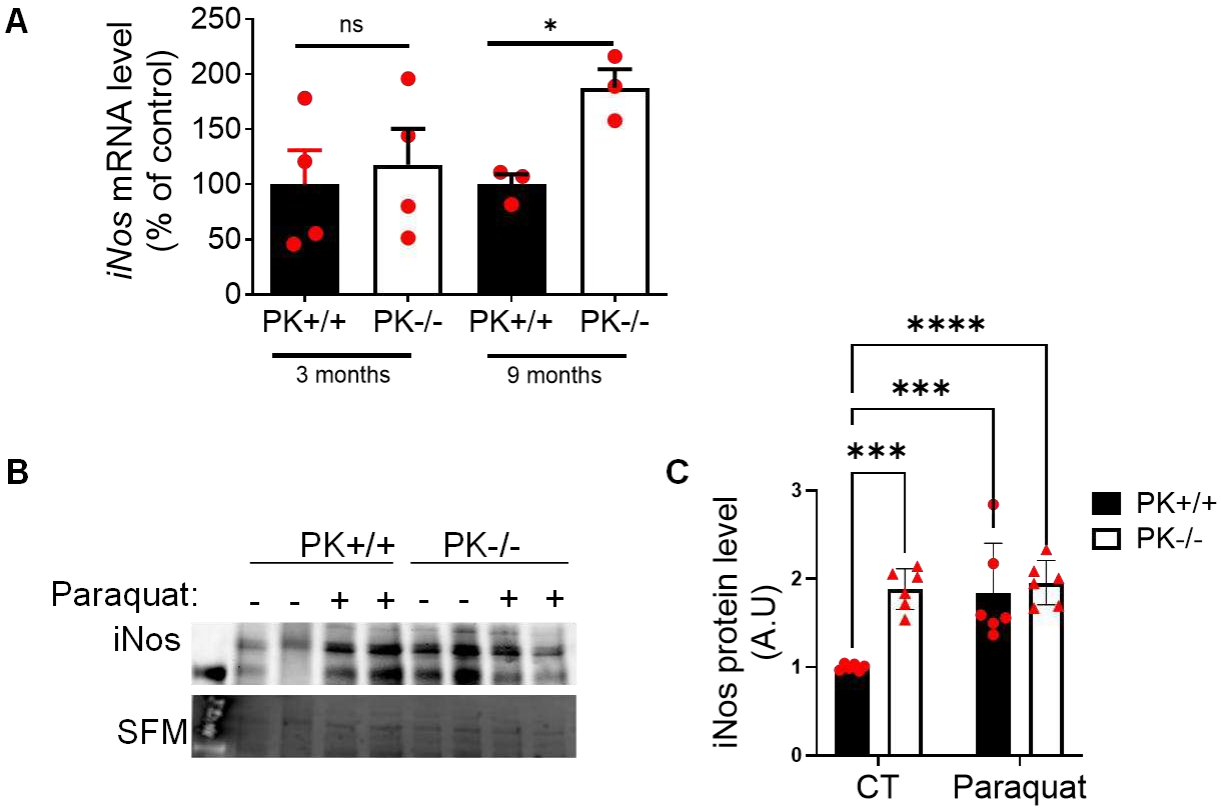


Figure 7 PK controls iNOS *in vivo* and this regulation is abolished by paraquat**.**

(A) RT-PCR analysis of the impact of endogenous PK depletion on *iNOS* mRNA levels in basal conditions in 3 (N = 4, Shapiro normality and Welch's t test) and 9 months (N = 3, Shapiro normality and Welch's t test) aged-mice as described in methods. **(B, C**) Analysis of PK knockout impact on iNOS protein levels in basal (saline, (-) and paraquat- (10 mg/kg, (+)) treated conditions) by Western blot in 9 month aged-mice as described in Methods. (**A**) Representative images of parkin and iNOS expressions analyzed by Western blot and normalized by total protein load per lane (stain free membrane, SFM). (**B**, N = 6, Two-way ANOVA) quantification analysis of iNOS expression in the striatum of wild-type (PK+/+) and KO PK (PK-/-) 9 month-aged mice in basal (CT) and paraquat treated conditions. Bars correspond to the means +/- SEM. *** $p < 0.001$ and **** $p < 0.0001$.

Supplementary Files

This is a list of supplementary files associated with this preprint. Click to download.

- uncroppedgels.pdf